# Rational Design of Self-Cleaving pre-tRNA–Ribonuclease P RNA Conjugates†

Daniel N. Frank, Michael E. Harris, and Norman R. Pace*

*Department of Biology, Indiana University, Bloomington, Indiana 47405*

*Received April 6, 1994; Revised Manuscript Received June 3, 1994®*

ABSTRACT: Ribonuclease P (RNase P) generates the mature 5′ end of tRNAs by removing 5′ leader sequences from pre-tRNAs. In vitro, the RNA subunit is sufficient to catalyze this reaction and is therefore a ribozyme. The kinetic analysis of RNase P-mediated catalysis is complicated because product release is normally rate-limiting. Furthermore, the intermolecular nature of the cleavage reaction precludes many applications of in vitro selection schemes to the analysis of RNase P. To examine and manipulate the RNase P function more effectively, we designed a pair of ribozymes in which the RNase P RNA is covalently linked to a pre-tRNA substrate. To facilitate intramolecular cleavage, pre-tRNA molecules were tethered to circularly permuted RNase P RNA molecules at nucleotides implicated in substrate binding. These "active-site-tethered" pre-tRNA–RNase P RNA conjugates undergo accurate and efficient self-cleavage in vitro, with first-order reaction rates equivalent to the rate of the chemical step of the native RNase P reaction. Unlike most ribozymes, RNase P recognizes its substrate through tertiary RNA–RNA interactions, rather than through extensive Watson–Crick base-pairing. However, the development of the active-site-tethered conjugates has led us to create a sequence-specific endonuclease, termed Endo.P. In the Endo.P configuration, the 3′ half of the pre-tRNA acceptor stem binds exogenous RNA substrates via Watson–Crick base-pairing; the bound substrate is subsequently cleaved at the predicted site. The demonstration of sequence-specific cleavage by Endo.P expands the potential of RNase P and its derivatives as reagents in gene therapy.

Ribonuclease P (RNase P) removes 5′ leader sequences from pre-tRNAs. The enzyme has been identified in organisms representing all three primary phylogenetic domains: Bacteria, Archaea, and Eucarya (Woese, 1990). Bacterial RNase P enzymes, particularly those of *Bacillus subtilis* and *Escherichia coli*, have been analyzed most extensively. Bacterial RNase P functions, in vivo, as a holoenzyme composed of single protein and RNA subunits (Pace & Smith, 1990; Altman et al., 1993). The RNase P RNA subunit functions catalytically in vitro in the absence of the protein subunit and thus represents an RNA enzyme, or ribozyme (Guerrier-Takada et al., 1983). Unlike all other characterized ribozymes (i.e., groups I and II autocatalytic introns, hammerhead, hairpin, and hepatitis delta virus), RNase P acts in trans in its native form to carry out multiple-turnover reactions. Furthermore, RNase P binds pre-tRNAs by interactions with elements of tertiary structure, rather than by extensive Watson–Crick base-pairing. Thus, the native RNase P ribozyme mainly recognizes substrate *structure* instead of *sequence* per se.

The intermolecular nature of the RNase P reaction presents several challenges to the study of RNase P structure and function. One consideration is that the rate-limiting step in pre-tRNA cleavage is the release of product, rather than the chemical step (i.e., bond breaking and making), under substrate-saturated conditions (Reich et al., 1988; Tallsjö & Kirsebom, 1993). This complicates kinetic and mutational analyses of RNase P-mediated catalysis because multiple-turnover reaction rates are dominated by substrate binding and product release rather than by the chemical process. Although reaction conditions have been described in which chemistry is rate-limiting (e.g., in the presence of $Ca^{2+}$ instead of $Mg^{2+}$ or at low pH; Smith & Pace, 1993), these nonnative conditions are less than ideal for the study of RNase P enzymology. Another challenge to the study of RNase P is that it is not altered by the cleavage reaction. Consequently, potentially informative strategies such as in vitro selection are not applicable to this system because they require the separation of functional and nonfunctional pools of molecules (Gold et al., 1993; Szostak & Ellington, 1993).

One way to avoid the constraints imposed by this intermolecular reaction is to covalently link the RNase P RNA to its pre-tRNA substrate, thus creating a self-cleaving ribozyme (Kikuchi et al., 1993; Waugh and Pace, unpublished). When pre-tRNA is linked to either the 5′ or 3′ terminus of RNase P, intramolecular cleavage can be achieved, but it is both inefficient and inaccurate. Indeed, intermolecular cleavage, rather than true self-cleavage, prevails under most reaction conditions when the pre-tRNA is linked to the native termini of RNase P (Kikuchi et al., 1993). The self-cleavage reaction is probably inefficient because the termini of RNase P, to which the substrate is linked, are not positioned near the active site of the ribozyme in three-dimensional space (Harris et al., 1994). Therefore, the tethered pre-tRNA substrate, unlike a pre-tRNA free in solution, has limited access to the active site. In principle, increasing the length of the nucleotide segment linking the pre-tRNA to RNase P could ameliorate such steric constraints, but this modification also favors intermolecular cleavage.

To facilitate the efficiency and accuracy of intramolecular cleavage, we constructed ribozyme–substrate conjugates in which the pre-tRNA substrate is positioned at the active site of RNase P. Although the precise nucleotides that constitute this active site are currently unknown, the secondary structure of bacterial RNase P RNA is well-established (James et al., 1988; Brown & Pace, 1992; Haas et al., 1994). Moreover,

† This work was supported by American Cancer Society Postdoctoral Fellowship PF-3933 (D.N.F.), National Institutes of Health Postdoctoral Fellowship GM 15979 (M.E.H.), and NIH Grant GM 34527 (N.R.P.).

* Corresponding author: Telephone, (812) 855-6152; FAX, (812) 855-6705; electronic mail address, nrpace@crab.bio.indiana.edu.

® Abstract published in *Advance ACS Abstracts,* August 1, 1994.

0006-2960/94/0433-10800$04.50/0 © 1994 American Chemical Society

intermolecular cross-linking and chemical footprinting studies have identified regions of RNase P RNA that are in close proximity to specific nucleotides in the bound substrate pre-tRNA (Burgin & Pace, 1990; Nolan et al., 1993; Oh & Pace, submitted for publication; LaGrandeur & Pace, 1994). Specific positioning of the substrate within a conjugate can be accomplished by fusing a pre-tRNA gene to a circularly permuted RNase P gene. A circularly permuted RNA is created by rearranging the RNase P RNA gene so that new 5′ and 3′ ends are formed at adjacent nucleotides within the RNase P RNA primary structure. Thus, novel 5′ and 3′ ends can be created at any pair of nucleotides within the RNase P RNA, and the tRNA gene can be appended to either end of the resulting molecule. Kinetic analyses demonstrate that disruption of the phosphodiester backbone of RNase P usually does not alter enzymatic activity to a significant extent (Reich et al., 1986; Guerrier-Takada & Altman, 1992; Waugh & Pace, 1993; Harris et al., 1994), so there is considerable flexibility in the design of tethered molecules. With this emerging structural perspective, it is now possible to generate enzyme–substrate conjugates in which the appropriate phosphodiester bond is poised at the ribozyme's active site.

In this paper, we describe the design and characterization of two "active-site-tethered" molecules that undergo efficient and accurate self-cleavage in vitro. Both conjugates undergo self-cleavage at rates that are comparable to the rate of bond cleavage in the native RNase P reaction. As an application of tethered RNase P technology, we have remodeled the active-site structure of a pre-tRNA–RNase P RNA conjugate to create a sequence-specific endoribonuclease. In this configuration, a fragment of the pre-tRNA functions as an Internal Guide Sequence (Davies et al., 1982) that binds exogenous RNA substrates via Watson–Crick base-pairing. This, in effect, converts a *structure*-specific ribozyme into a *sequence*-specific ribozyme. Such RNase P derivatives may prove to be useful reagents for ribozyme-based gene therapy (Rossi & Sarver, 1990; Altman, 1993).

## MATERIALS AND METHODS

*Oligonucleotides.* PT292 Forward: CGG GAT CCG GTA GGC TGC TTG AGC CAG T. PT292 Reverse: GAA GAT CTA CGG GTT CAG TAC GGG CCG T. ECG332 Forward: TAA TAC GAC TCA CTA TAG AAT GAC TGT CCA CGA CAG. ECG332 Reverse: ATC TAG GCC AGC AAT CG. PRE.1: GAT CCT ACC GGA CCA TTT TGG GTA C. ANTI-PRE.1: CCA AAA TGG TCC GGT AG. PRE.2: GAT CCT GAA CTA CCG GAC CAT TTT GGG TAC. ANTI-PRE.2: CCA AAA TGG TCC GGT AGT TCA G. ENDO.1: CGG AAT TCT AAT ACG ACT CAC TAT AGT TCA GTT GGT TAG AAT GCC. ENDO.2: CGG AAT TCT AAT ACG ACT CAC TAT AGT TGG TTA GAA TGC CTG CC. 52R: CCG CGA CCT CCT GCG TG.

*Plasmids.* The following plasmids were used in this work: pUC18 was purchased from New England Biolabs. pDW98, pDW128, and pDW152 were provided by D. Waugh (1989). pDS153F was provided by D. Smith (D.S. and N.R.P., unpublished). pBST-mBsD-CCA and p153Bsttan were provided by J. Nolan (1993).

*Cloning.* Construction of circularly permuted RNase P RNA genes (e.g., CP292 and CP332) followed Nolan et al. (1993) and is described elsewhere, along with a kinetic analysis of these RNAs (Harris et al., 1994). Plasmid pTP5 was constructed by inserting the *Bam*HI/*Xho*I fragment of DW98 that carries the native RNase P gene into the *Bam*HI/*Sal*I sites of pDW152. Plasmid pTP292 was constructed by inserting a *Bam*HI/*Bgl*II-digested polymerase chain reaction (PCR) fragment, which carries CP292, into the *Bam*HI site of pDS153F. Plasmid pPT332 was constructed by first inserting a PCR fragment carrying CP332 into the *Sma*I site of pUC18 to create pMEH1. The *Kpn*I/*Nlu*I fragment of pDW128, which carries the pre-tRNA$^{Asp}$ gene, was subsequently ligated into the *Kpn*I and *Nar*I sites of pMEH1 to create pPT332.

Endo.P1 and Endo.P2 genes were synthesized by PCR of pTP292 with oligos ENDO.1 or ENDO.2 as forward primers and PT292 Reverse as the reverse primer. PCR fragments were digested with *Eco*RI and *Bgl*II then inserted into the *Eco*RI and *Bam*HI sites of plasmid p153Bsttan to create pENDO.1 and pENDO.2. Substrate RNA genes were constructed by ligating annealed pairs of oligonucleotides (PRE.1 + ANTI-PRE.1 or PRE.2 + ANTI-PRE.2) encoding the precursor sequences into the *Kpn*I and *Bam*HI sites of plasmid pDS153F to create plasmids pPRE.1 and pPRE.2. Oligonucleotides were annealed and subsequently purified following the protocol of Frank et al. (1994).

*Preparation of RNA Transcripts.* RNAs were synthesized in vitro by run-off transcription using T7 RNA polymerase (gift of B. Pace). Transcription reactions followed the protocol of Milligan and Uhlenbeck (1989), except that the NTP concentration was raised to 5 mM. RNAs were radiolabeled internally by the addition of 50 μCi of [α-$^{32}$P]GTP to the transcription mix; the concentration of unlabeled GTP was lowered to 0.2 mM in these reactions. Transcription reactions of tethered RNAs were carried out at 25 °C, rather than at 37 °C, to minimize self-cleavage. Transcription products were phenol/chloroform-extracted twice, ethanol-precipitated, and loaded onto a 6% polyacrylamide/7 M urea gel. Following gel electrophoresis, RNAs were visualized by either UV shadow or autoradiography. The appropriately sized bands were excised, and RNA was eluted from the gel slices by passive diffusion (overnight, 25 °C) into a buffer consisting of 0.3 M sodium acetate, 10 mM Tris Cl (pH 7.4), 1 mM EDTA, and 0.5% SDS. The RNA eluate was extracted once with phenol/chloroform and once with chloroform before ethanol precipitation. Pelleted RNA was resuspended in $H_2O$ and quantitated by either UV absorbance (260 nm) or specific radioactivity.

RNAs were synthesized from the following linearized plasmids (the restriction enzyme used to digest each plasmid is listed parenthetically): (1) pre-tRNA$^{Asp}$-pDW152 (*Bst*NI); (2) native RNase P RNA-pDW98 (*Sna*BI); (3) mature tRNA$^{Asp}$-pBST-mBsD-CCA (*Bst*NI); (4) TP5-pTP5 (*Fok*I); (5) TP292-pTP292 (*Fok*I); (6) PT332-pPT332 (*Bst*NI); (7) Endo.P1-pENDO.1 (*Fok*I); (8) Endo.P2-pENDO.2 (*Fok*I); (9) Pre.1-pPRE.1 (*Fok*I); (10) Pre.2-pPRE.2 (*Fok*I).

*Cleavage Assays.* Unless otherwise noted, all cleavage reactions were conducted in a buffer of 16.5 mM PIPES, 44 mM Tris Cl (pH 8.0), 0.1% SDS, 3 M ammonium acetate, and 25 mM magnesium chloride (Smith & Pace, 1993). To accurately measure rate constants for the TP292 and PT332 reactions, cleavage reactions were carried out at pH 6.0, and sodium chloride was substituted for ammonium acetate (Smith & Pace, 1993). For the dilution experiments (Figure 2, Table 1), equivalent quantities of enzyme were diluted into either 4- or 400-μL reaction mixes to give final RNA concentrations of 2 or 0.02 nM, respectively (substrate was similarly diluted in the native RNase P reactions). In the tRNA inhibition experiments, RNA concentrations were as follows: 2 nM

enzyme, 2 nM substrate (for the native RNase P reaction), and 50, 250, or 1250 nM unlabeled competitor tRNA. Endo.P reactions employed 100 nM enzyme and 100 nM substrate.

In all cleavage reactions, enzyme and substrate RNAs were mixed in reaction buffer (minus magnesium chloride) on ice, heated for 5 min at 65 °C, and then shifted to the reaction temperature, 50 °C. Reactions were initiated by the addition of prewarmed magnesium chloride and quenched, after the indicated times, by the addition of 3 vol of ice-cold ethanol, 1–2 vol of 50 mM EDTA, and 4 μg of glycogen. Following precipitation, precursor and product RNAs were resolved by electrophoresis through denaturing 6% polyacrylamide/7 M urea gels. Precursor and product RNA levels were quantitated by phosphorimager analysis (Molecular Dynamics) of dried gels.

Reaction rate constants for the TP5, TP292, PT332, and native RNase P reactions were obtained by measuring the extent of cleavage as a function of time. The apparent rate constant, $k_{app}$, is given by the slope of a plot of $\ln(S_0/S_t)$ versus time, where $S_0$ equals the initial substrate concentration and $S_t$ equals the substrate concentration at a given time point (Segal, 1975). Three to four separate cleavage time courses were performed for each enzyme dilution, and slopes were calculated by linear regression.

*Assessment of Cleavage Accuracy.* TP292 and PT332 large-scale (0.4 mL) cleavage reactions were performed as described above with a ribozyme concentration of 1 nM. For the large-scale native RNase P reaction, the ammonium acetate concentration was lowered to 1 M, and the reaction was incubated at 37 °C for 1 h. Final enzyme and substrate concentrations were 10 nM. Reactions were quenched by ethanol precipitation. Primer extension analysis of reaction products followed the protocol of Burgin et al. (1990) and used the $tRNA^{Asp}$-specific oligonucleotide 52R (Nolan et al., 1993).

For terminal nucleotide analysis, aliquots of the large-scale reactions were labeled with [5′-$^{32}$P]cytidine bisphosphate (pCp) and T4 RNA ligase (England et al., 1980), and the 5′ products of the cleavage reactions were gel-purified. RNAs were hydrolyzed with 0.04 N NaOH (37 °C overnight) and neutralized with HCl, and the resulting 3′ nucleoside monophosphates were resolved by two-dimensional thin-layer chromatography on 13254 cellulose (Kodak) following the protocol of Nishimura (1979). The solvents used in chromatography were as follows: (1) first dimension, 5:3 isobutyric acid/0.5 M NaOH; (2) second dimension, 70:15:15 isopropyl alcohol/HCl/$H_2O$. The migration of unlabeled 3′ nucleoside monophosphates, added as markers, was monitored by UV shadow.

## RESULTS

*Design of Tethered pre-tRNA–RNase P Molecules.* The pre-tRNA–RNase P RNA conjugates examined in this study are shown in Figure 1 (see Materials and Methods for the details of construction). All tethered molecules consist of *E. coli* RNase P RNA joined to *B. subtilis* pre-$tRNA^{Asp}$. In construct TP5, pre-tRNA was linked to nucleotide 5 of RNase P RNA (in our nomenclature PT indicates a tRNA linked to the 3′ end of RNase P, while TP indicates a tRNA linked to the 5′ end of RNase P; the numeral specifies the native nucleotide at the 5′ end of the circularly permuted RNase P). Since the 5′ and 3′ ends of RNase P RNA are remote from the active site (Harris et al., 1994), we expected that tight linkage of substrate to the 5′ end of RNase P would not result in efficient self-cleavage (Kikuchi et al., 1993). TP5 is thus a negative control for comparison with conjugates tethered at the active site. The rationale for the design of two active-site-tethered molecules, TP292 and PT332, is as follows.

Nucleotide G292 of RNase P was selected as a conjugation site for the 3′ terminus of pre-tRNA because this nucleotide is adjacent to the 3′ end of tRNA in the native ribozyme–substrate complex. Indeed, G292 is cross-linked by pre-tRNA modified with a 3′ photoaffinity agent (Oh & Pace, submitted for publication). In addition, pre-tRNA protects G292 from chemical modification (Knap et al., 1990), and this protection requires the presence of the tRNA 3′ terminal CCA sequence (LaGrandeur et al., 1994). TP292 was constructed by fusing the 3′ end of pre-tRNA, by a 6 nucleotide linker, to the 5′ end of a circularly permuted RNase P gene that begins at position G292 (Figure 1).

The design of PT332 RNA was based on similar criteria. Mature tRNA carrying a cross-linking agent attached to its 5′-phosphate, the phosphate acted upon by RNase P, cross-links to two regions of RNase P RNA, one of which includes nucleotide G332 (Burgin & Pace, 1990). In addition, bound pre-tRNA specifically protects G332 of RNase P RNA from chemical modification, but mature tRNA does not (LaGrandeur et al., 1994), indicating that the 5′ leader sequence of pre-tRNA is juxtaposed to G332 in the native enzyme–substrate complex. Therefore, we fashioned PT332 by linking pre-tRNA sequences to a circularly permuted RNase P RNA that begins at position G332. A 13-nucleotide linker separates the cleavage site in tRNA and RNase P sequences (Figure 1).

*Initial Characterization of Cleavage Reactions.* Tethered RNAs were synthesized by in vitro run-off transcription using T7 RNA polymerase and purified by denaturing gel electrophoresis (Milligan & Uhlenbeck, 1989). In all experiments, RNAs were heated to 65 °C in reaction buffer lacking $Mg^{2+}$ for 5 min to allow renaturation and then were shifted to reaction temperature for 5 min before the addition of $Mg^{2+}$ to initiate the reaction (samples were diluted prior to preincubation to minimize the dimerization of tethered RNAs).

One hallmark of a self-cleavage reaction is that the rate of reaction is expected to be independent of enzyme concentration. In contrast, the rate of an intermolecular cleavage reaction is expected to be proportional to enzyme concentration at subsaturating substrate concentration. Figure 2 shows a gel analysis of the reaction products of native and tethered RNase P RNAs at different RNA concentrations. At a concentration of 2 nM, all tethered RNAs undergo cleavage to varying extents (Figure 2; note that in Figure 2, TP292 and PT332 molecules were reacted for 15 min while native RNase P and TP5 were reacted for 60 min). At 0.02 nM, however, both the native RNase P and TP5 reaction rates are significantly decreased, whereas the extents of the TP292 and PT332 reactions are unaffected. This suggests (but does not prove, see below) that TP292 and PT332 RNAs mainly cleave intramolecularly.

The accuracy of cleavage by the tethered RNAs can be judged by comparison of the reaction products to those of the standard intermolecular reaction, in which pre-tRNA is cleaved to form a 77-nt (nucleotide) mature tRNA and a 33-nt 5′ leader sequence. As predicted, cleavage of RNAs TP5 and TP292 produces a fragment that comigrates with the 5′ leader sequence and a product that runs just below the uncleaved precursor. PT332 also generates the products expected from the use of the authentic cleavage site: mature tRNA (77 nt) and a longer fragment corresponding to RNase P. The multiple mature tRNA fragments produced in the

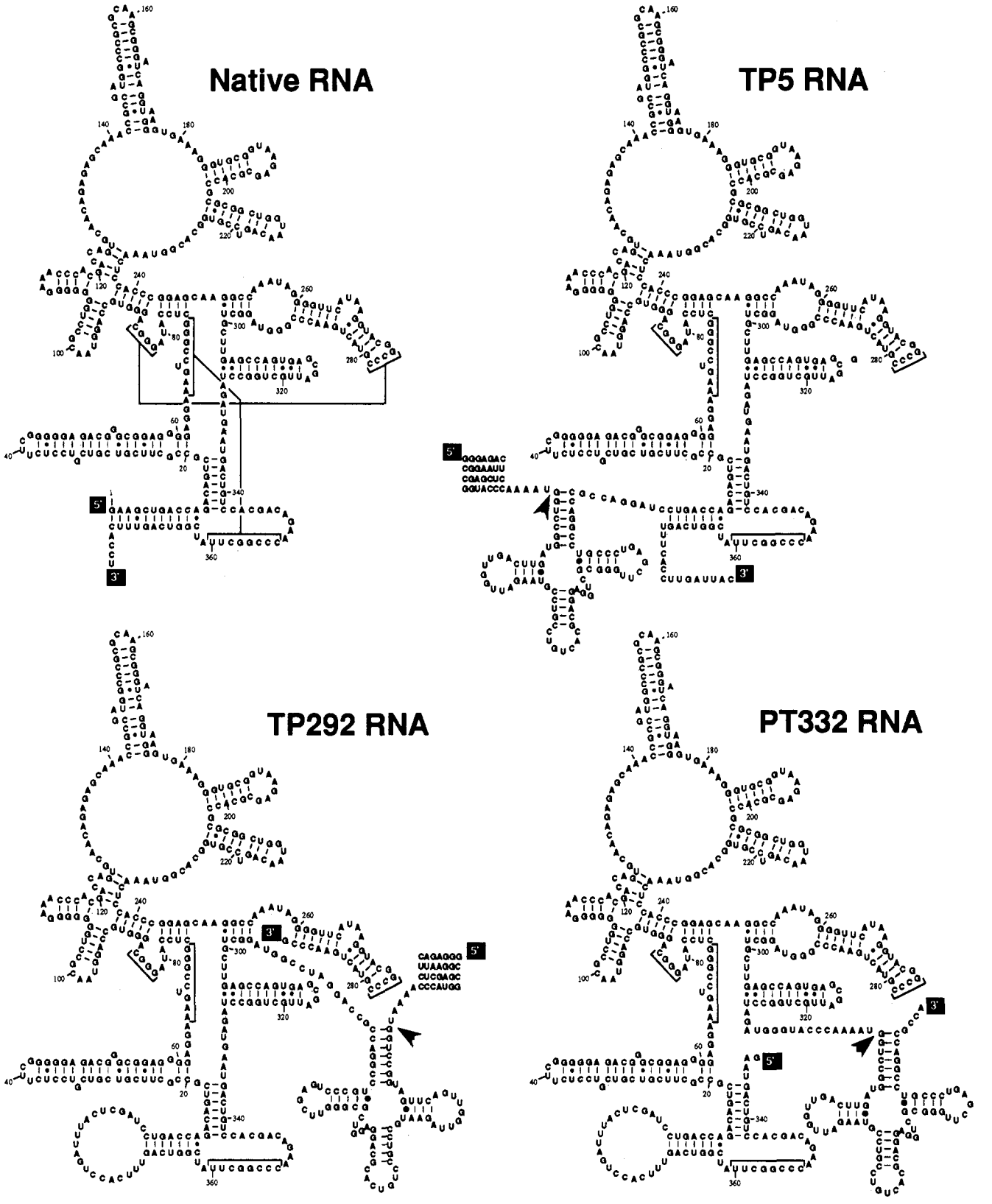


FIGURE 1: Secondary structures of native RNase P and tethered pre-tRNA–RNase P conjugates. Arrows denote predicted sites of endonucleolytic cleavage.

PT332 cleavage reaction are due to 3′ terminal heterogeneity in the precursor, generated during in vitro transcription (Milligan & Uhlenbeck, 1989), rather than miscleavage (below).

The optimal reaction conditions for both TP292 and PT332 were found to be 2.5–3.0 M ammonium acetate and 25 mM magnesium chloride with incubation at 50 °C. Omission of the 65 °C preincubation step dramatically decreased cleavage efficiency. Under these conditions, typically 60–90% of input TP292 or PT332 RNAs are cleaved rapidly (within 15 min), whereas the extent and rate of the TP5 cleavage reaction are impaired significantly (see below). The requirement of high ionic strength for efficient cleavage by TP292 and PT332 may reflect increased structural flexibility at low ionic strength,

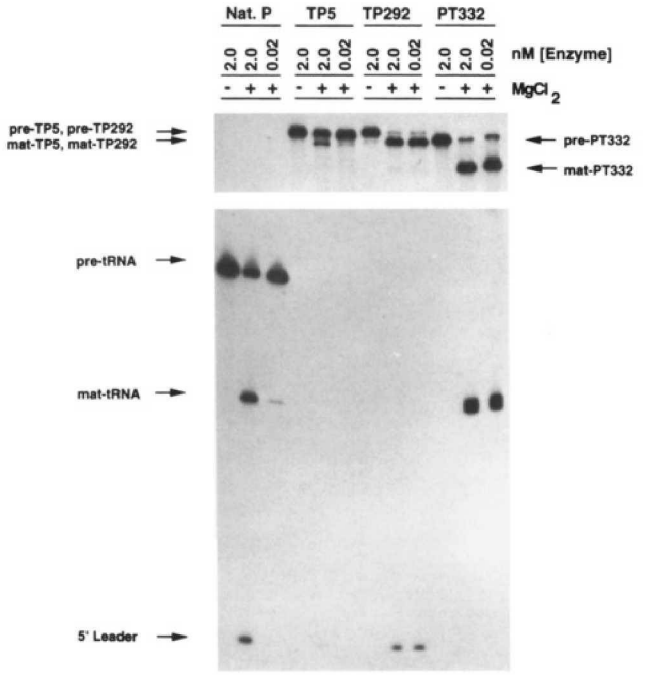


FIGURE 2: Tethered cleavage assays. As detailed in Materials and Methods, labeled RNAs were incubated in reaction buffer (16.5 mM PIPES, 44 mM Tris Cl (pH 8.0), 0.1% SDS, and 3 M ammonium acetate) at 50 °C for either 60 min (native RNase P and TP5) or 15 min (TP292 and PT332), in either the presence or absence of 25 mM $MgCl_2$. Reaction precursors and products were separated by denaturing 6% polyacrylamide gel electrophoresis. Equivalent quantities of enzyme were diluted into either 4- or 400-$\mu$l reaction mixtures to give final RNA concentrations of 2 or 0.02 nM, respectively (substrate was diluted similarly in the native RNase P reactions). Nat. P: native RNase P reaction.

a consequence of interrupting the core structure of the ribozyme by insertion of the substrate. Circularly permuted RNase P RNAs commonly require higher ionic strengths for optimal activity than does the native RNA (Harris et al., 1994). High monovalent cation concentrations presumably decrease unfavorable, repulsive ionic forces and/or increase stabilizing hydrophobic interactions such as base-stacking. The requirement for TP292 and PT332 of higher temperature than is optimal for the native RNase P reaction may indicate a tendency of PT332 and TP292 to form alternative, noncatalytic structures; elevated temperature may promote formation of the native (catalytic) form of the enzyme–substrate complex.

*TP292 and PT332 Cleavage Is Accurate.* The cleavage sites used by TP292 and PT332 were mapped more precisely by primer extension analysis of the 3′ products and 3′ terminal nucleotide analysis of the 5′ products. Figure 3a shows primer extension analyses of the cleavage products of unlabeled native RNase P, TP292, and PT332 RNAs using oligonucleotide primers complementary to tRNA. Run-off transcripts map the 5′ ends of the processed tRNA molecules and correspond to the authentic RNase P cleavage site for both TP292 and PT332. Minor extension products one nucleotide longer than the prominent band were seen in all products. This could be due to a low frequency of miscleavage or, more likely, to the nonspecific addition by reverse transcriptase of nonencoded nucleotides to the 3′ ends of run-off transcripts (Clark, 1988). Miscleavage that results in a longer 3′ product predicts a similarly shortened 5′ product, a hypothesis that we tested by 3′ terminal nucleotide analysis. The 5′ products that result from cleavage of TP292 (i.e., 5′ leader) and PT332 (i.e., cleaved RNase P) were isolated, and the 3′ terminal nucleotide of

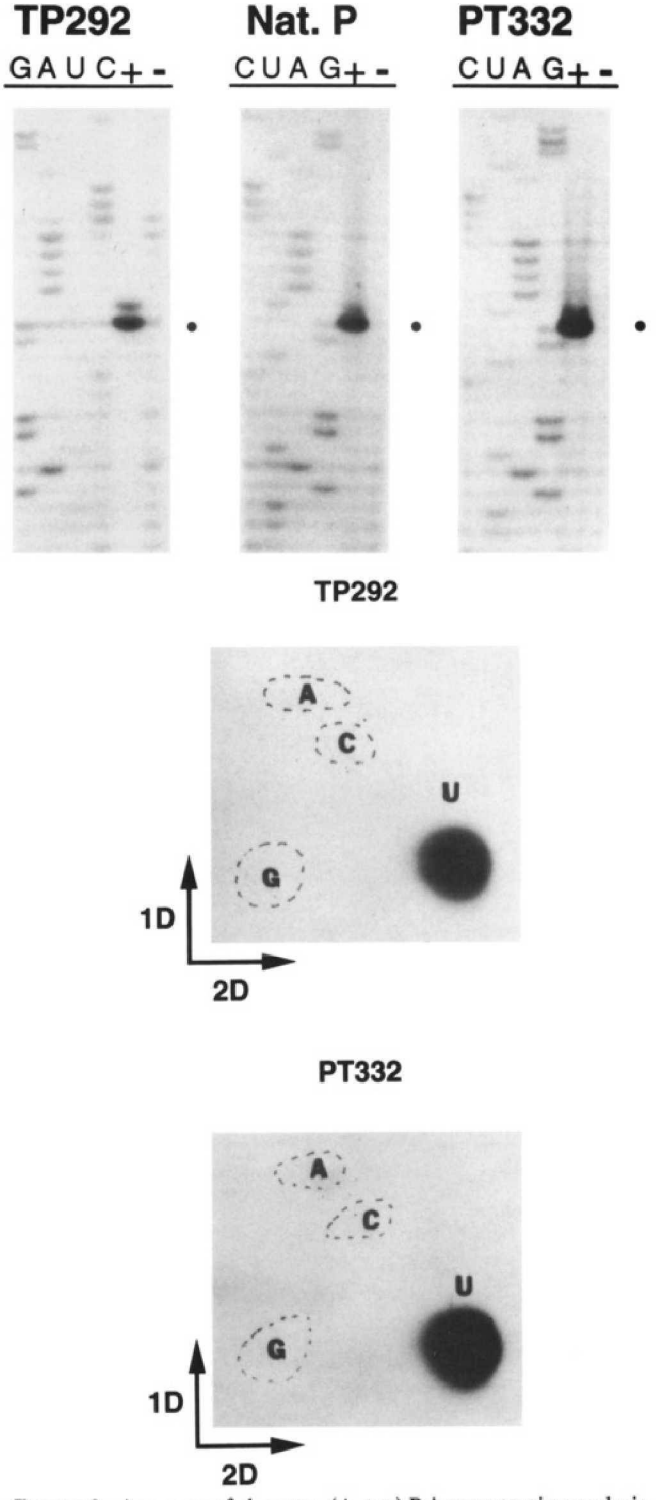


FIGURE 3: Accuracy of cleavage. (A, top) Primer extension analysis of gel-purified 3′ products of TP292, PT332, and native RNase P cleavage (Materials and Methods). Predicted cleavage sites are marked by closed circles. G, A, T, C: RNA sequencing lanes. +: cleaved RNA. –: uncleaved RNA. (B, bottom) 3′ terminal nucleotide analysis of 5′ products of TP292 and PT332 cleavage. Gel-purified products were labeled with [5′-$^{32}$P]-3′-cytidine bisphosphate (pCp), hydrolyzed with alkali, and 3′ nucleoside monophosphates (NMPs) were separated by two-dimensional thin-layer chromatography. Unlabeled 3′ NMPs were included in the TLC and identified by UV shadow. The predicted 3′ nucleotide in both TP292 and PT332 cleavage is 3′-UMP.

each product was determined (described in Materials and Methods). More than 99% of the 3′ termini of both samples corresponded to the nucleotide (U) expected for cleavage at the authentic RNase P cleavage site (Figure 3B). Both TP292

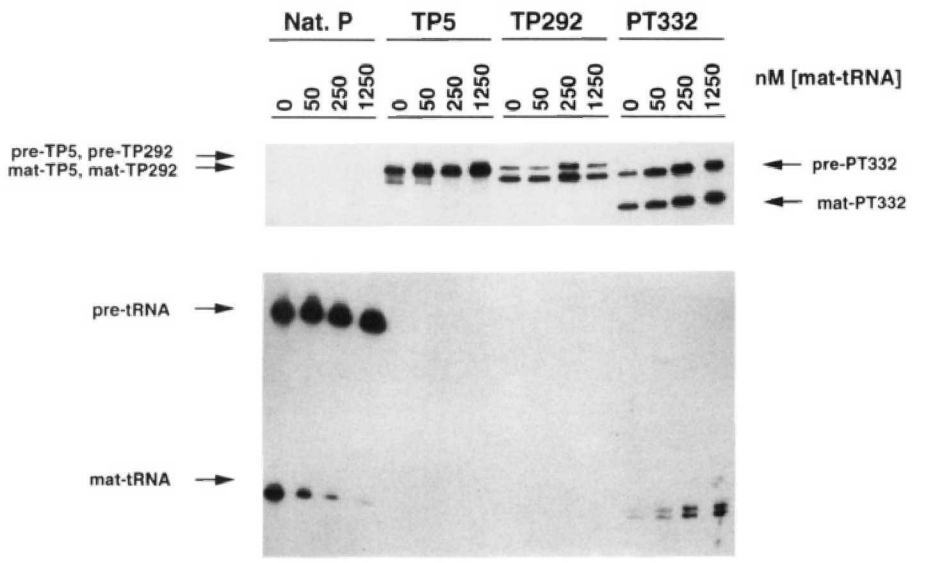


FIGURE 4: Inhibition of cleavage by mature competitor tRNA. Reaction conditions were the same as for Figure 2, with the addition of the indicated concentrations of nonradioactive, mature tRNA. The final concentration of enzyme (and radioactive pre-tRNA in the native RNase P reactions) was 2 nM in each reaction. Nat. P: native RNase P reaction.

Table 1: Apparent Rate Constants at Two Enzyme Concentrations

| | $k_{app}$ (min$^{-1}$)[c] | |
|---|---|---|
| sample | 2 nM [E] | 0.02 nM [E] |
| native[a] | 0.013 ± 0.0013 | 0.00038 ± 0.00012 |
| TP5[a] | 0.0032 ± 0.0015 | 0.00022 ± 0.00012 |
| TP292[b] | 1.2 ± 0.37 | 1.5 ± 0.26 |
| PT332[b] | 1.3 ± 0.20 | 1.2 ± 0.18 |

[a] Assayed at pH 8.0 (see Materials and Methods). [b] Assayed at pH 6.0 (see Materials and Methods). [c] Measured as the slope of ln(% uncleaved) versus time. For an intermolecular reaction, $k_{app} = (k_{cat}/K_m)[E]$. For an intramolecular reaction, $k_{app}$ is the exponential decay constant. Values are reported as mean ± standard deviation.

and PT332 thus exhibit precise cleavage of the appropriate phosphodiester bond.

*Active-Site-Tethered RNAs Efficiently Self-Cleave.* The results presented in Figure 2 suggest, but do not prove, the hypothesis that TP292 and PT332 undergo self-cleavage. To more rigorously address the question of self-cleavage by TP292 and PT332, we determined the effect of dilution upon the apparent reaction rate constant, $k_{app}$, for each of these conjugates, as well as for TP5 and the native reaction. Again, in an intramolecular reaction, $k_{app}$ is expected to be insensitive to dilution of reactants. Under optimal reaction conditions, the rates of TP292 and PT332 cleavage were too fast to measure accurately; assays with these RNAs were performed, therefore, under conditions known to slow the native RNase P RNA chemical reaction rate. Previous analysis of the native RNase P reaction showed that reducing the pH from 8.0 to 6.0 causes an approximately 100-fold reduction in the rate of catalysis in single-turnover reactions (Smith & Pace, 1993); indeed, under low pH conditions it was possible to determine the rates of the TP292 and PT332 reactions. The apparent rate constants, $k_{app}$, for TP5, TP292, PT332, and native RNase P at 2 and 0.02 nM enzyme (and substrate) are summarized in Table 1. The rate constants for both TP292 and PT332 are independent of RNA concentration, within the range tested. The insensitivity of $k_{app}$ to the concentration of reactants clearly demonstrates that the TP292 and PT332 tethered molecules undergo self-cleavage. In contrast, both the native RNase P and TP5 reaction rates are decreased significantly upon 100-fold dilution of the ribozymes.

As a final test of self-cleavage, native RNase P, TP5, TP292, and PT332 reactions were assayed for inhibition by mature tRNA. Mature tRNA is a competitive inhibitor of the intermolecular RNase P reaction (Reich et al., 1988; Smith et al., 1992), but would not be expected to interfere with an intramolecular reaction because the tethered substrate already occupies the active site of the ribozyme. As shown in Figure 4, both the native RNase P RNA and TP5 reactions are inhibited by unlabeled competitor tRNA. In contrast, neither the TP292 nor the PT332 reaction was significantly affected by competitor tRNA concentrations as high as 1250 nM (ca. $50K_m$ for native RNase P; Smith & Pace, 1993). This insensitivity of the TP292 and PT332 reactions to inhibition by tRNA is further indication that these reactions occur in cis.

*Remodeling RNase P Substrate Specificity.* Previous work with model RNase P substrates demonstrated that the native ribozyme is capable of cleaving RNA duplexes that mimic the structure of the tRNA acceptor stem. For instance, Forster and Altman (1990) have designed short RNA oligomers, termed external guide sequences (EGS), that bind and fold target RNA sequences into structures that are cleaved by RNase P. Aside from complementarity between EGS and target sequences, the only other requirement for RNase P-mediated cleavage is that the 3′ termini of EGS RNAs must consist of the trinucleotide CCA (Forster & Altman, 1990). The ability to tether tRNA substrates to RNase P thus also presents the possibility of tethering analogues of EGS sequences to RNase P to convert it from a structure-specific to a sequence-specific ribozyme.

To test this possibility, one of the active-site-tethered molecules, TP292, was modified to function as a sequence-specific endoribonuclease, termed Endo.P. Two such constructs, Endo.P1 and Endo.P2, were created by deleting 5′ segments of the tethered tRNA (Figure 5). In Endo.P1, the 5′ half of the acceptor stem was deleted (nt 1–9), while in Endo.P2 this deletion was extended through the 5′ half of the D stem (nt 1–14). We predicted that the tRNA sequences complementary to the deleted nucleotides (i.e., the 3′ sides of the acceptor and D stems) would be available to base-pair with exogenous RNAs bearing complementary sequences. In effect, the tRNA segments of the tethered ribozymes constitute internal guide sequences (IGS; Davies et al., 1982) for the

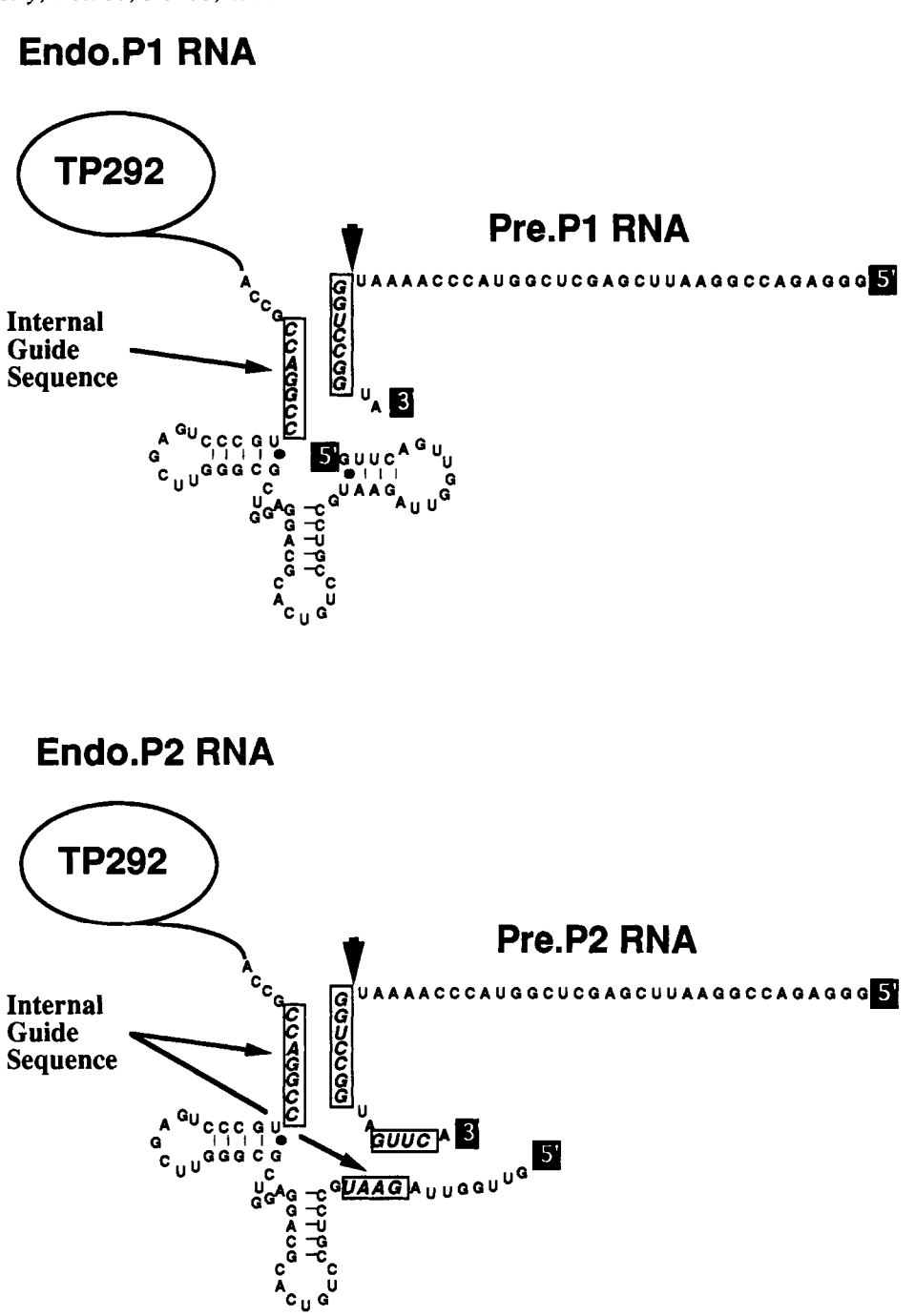


FIGURE 5: Design of sequence-specific RNase P derivatives, Endo.P. Secondary structures of the internal guide sequence-encoding regions of Endo.P1 and Endo.P2 are shown in detail, along with the sequences of their matched substrates. Arrows denote predicted sites of cleavage within the exogenous substrate RNAs.

recognition of exogenous RNA substrates.

The substrates for Endo.P1 and Endo.P2 consisted of 5′ leader sequences joined to sequences complementary to the respective IGS sequences (Figure 5). As shown in Figure 6, both Endo.P1 and Endo.P2 are capable of cleaving their complementary target RNA molecules. The optimal conditions for Endo.P cleavage are similar to those of TP292 self-cleavage (50 °C, 2.5–3.0 M ammonium acetate and 10 mM magnesium chloride). Under these conditions, the Endo.P reaction rates were significantly slower than the rate of TP292 self-cleavage. Presumably, the rate of Endo.P cleavage is limited by the substrate-binding step.

With both Endo.P1 and Endo.P2, cleavage occurs at the site predicted by the complementarity between the internal guide sequence and the substrate, as evidenced by the release of a product RNA that comigrates with the 5′ leader sequence generated in a native RNase P cleavage reaction. Thus, the substrate-binding specificity of RNase P has been altered to create a novel ribozyme that accurately recognizes its substrate by Watson–Crick base-pairing. Finally, both Endo.P1 and Endo.P2 are capable of cleaving RNA substrates with 3′ ends that extend beyond the regions of IGS complementarity (data not shown).

## DISCUSSION

In this paper, we have described the design and characterization of several ribozymes derived from the catalytic RNA subunit of RNase P. The first set of ribozymes consists of catalytic RNA molecules covalently linked to their substrate, pre-tRNA. Prior phylogenetic and biochemical analyses of native RNase P have provided considerable perspective on the structure of the ribozyme–substrate complex (Burgin &

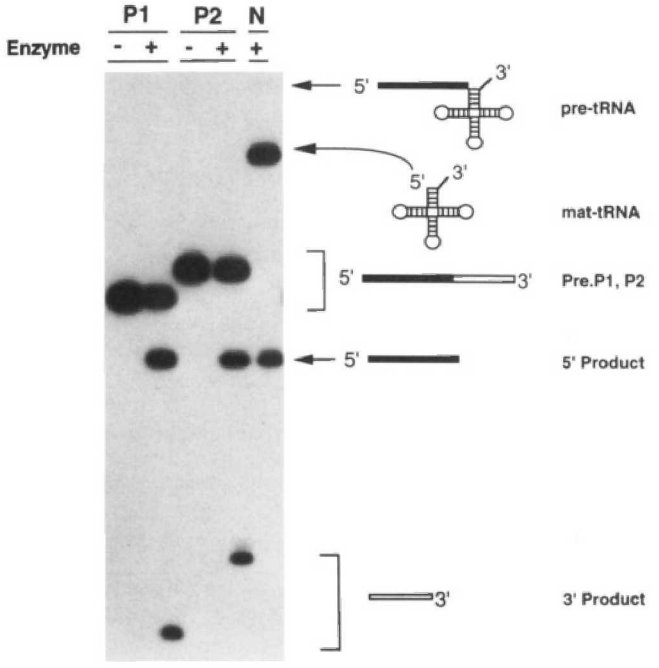


FIGURE 6: Site-specific intermolecular cleavage by Endo.P ribozymes. Internally labeled substrate RNAs (Pre.P1 and Pre.P2) were incubated with or without their respective ribozymes (Endo.P1 and Endo.P2). pre-tRNA$^{Asp}$ cleavage by native RNase P was included as a control of specific cleavage; cleavage of Pre.P1 and Pre.P2 is predicted to release a fragment identical to the 5′ leader sequence of pre-tRNA. Reaction conditions: 60 min, 50 °C, 16.5 mM PIPES, 44 mM Tris Cl (pH 8.0), 0.1% SDS, 2.5 M ammonium acetate, and 10 mM magnesium chloride. Reactions were 100 nM in both enzyme and substrate. P1: Pre.P1–Endo.P1 reaction. P2: Pre.P2–Endo.P2 reaction. N: native RNase P + pre-tRNA$^{Asp}$.

Pace, 1990; LaGrandeur et al., 1994; Oh & Pace, submitted for publication; Harris et al., 1994). We used this perspective to design pre-tRNA–RNase P conjugates in which the substrate is positioned in close proximity to the active site of the ribozyme. By tethering the pre-tRNA to circularly permuted RNase P molecules, the substrate could be linked to nucleotides of the ribozyme that are internal in the native RNA. Two sites of attachment, G292 and G332, were selected on the basis of the association of these nucleotides with, respectively, the 3′ and 5′ ends of tRNA.

The resulting tethered molecules, TP292 and PT332, undergo self-cleavage in vitro, as judged by two criteria. First, the apparent rate constants of the TP292 and PT332 cleavage reactions do not vary over a 100-fold range of enzyme concentrations; the rates of intermolecular reactions would be expected to fall upon dilution of the enzyme. In contrast, both the native RNase P and TP5 reactions exhibited decreases in $k_{app}$ upon dilution of the reactants. Second, TP292 and PT332 cleavage reactions are unaffected by the addition of up to 1250 nM competitor tRNA ($K_m$ for the native RNase P–tRNA interaction is approximately 50 nM; Smith & Pace, 1993); the native RNase P and TP5 reactions were both strongly inhibited by equivalent levels of competitor tRNA. These data do not formally rule out the possibility of intermolecular cleavage; however, such a reaction would require that the affinity of the enzyme for its substrate be several orders of magnitude higher than that of the native RNase P reaction to account for the insensitivity of the TP292 and PT332 reaction rates to the range of dilutions tested. We thus conclude that the TP292 and PT332 cleavage reactions occur primarily through self-cleavage, rather than intermolecular cleavage.

Kikuchi et al. (1993) have recently reported that tethered molecules similar to TP5 can undergo intramolecular cleavage to a limited extent. While our data do not absolutely exclude the possibility of TP5 self-cleavage, they do indicate that intermolecular cleavage predominates since the TP5 reaction rate is sensitive to both dilution and competition with competitor tRNA. An upper limit to the rate of TP5 self-cleavage (as opposed to intermolecular cleavage) can be estimated by the rate of cleavage measured at 0.02 nM TP5: $2.2 \times 10^{-4}$ min$^{-1}$. This rate is approximately 4 orders of magnitude slower than the rates measured for TP292 and PT332. Furthermore, the TP5 reaction often produced inaccurately cleaved products (data not shown), an effect that was also reported by Kikuchi et al. (1993) in their analysis of TP5-like RNAs.

One rationale for designing self-cleaving RNase P derivatives was that such molecules should not be rate-limited by product release, as is the native RNase P reaction. If instead the chemistry of the reaction were rate-limiting for self-cleavage, then the conjugates could be useful tools for examining the effects of mutations or other perturbations on the rate of the chemical step of catalysis. As summarized in Table 1, the first-order rate constants of the TP292 and PT332 self-cleavage reactions are 1.5 and 1.2 min$^{-1}$, respectively (values measured at 0.02 nM). These rates compare favorably to the rate of the chemical step of native RNase P RNA, 2.3 min$^{-1}$, measured by Smith and Pace (1993) under single-turnover conditions at pH 6.0. TP292- and PT332-catalyzed reactions therefore are likely to be limited by the rate of phosphodiester bond cleavage. Thus, the active-site-tethered conjugates should prove to be useful for studying catalysis by RNase P.

In addition to being fast compared to TP5 and native RNase P reactions, the TP292 and PT332 self-cleavage reactions are accurate. In both conjugates, greater than 99% of cleavage events occur at the appropriate phosphodiester bond, as judged by 3′ terminal nucleotide analysis (Figure 3). Both TP292 and PT332 self-cleavage reactions also are efficient: reactions normally proceeded to 60–90% completion. The speed, accuracy, and efficiency of TP292 and PT332 cleavage reactions all indicate that the substrate tRNA is tethered at or in close proximity to the active site of RNase P in both conjugates; the term "active-site tether" is indeed justified. Furthermore, highly efficient cleavage should prove to be advantageous for the application of in vitro selection schemes (Gold et al., 1993; Szostak & Ellington, 1993) to the further analysis of RNase P function; selection experiments utilizing tethered conjugates are in progress.

The TP292 conjugate was modified further to function as a sequence-specific endonuclease (Figures 5 and 6). In each of the two configurations tested, the 3′ half of the tRNA acceptor stem (as well as the D stem in construct Endo.P2) functioned as an internal guide sequence (IGS; Davies et al., 1982) that bound exogenous RNA substrates. Both Endo.P1 and Endo.P2 cleaved substrate RNAs at the positions predicted by the complementarity between their IGS sequences and the substrate RNAs. The absence of significant miscleavage indicates that Watson–Crick base-pairing allows highly sequence-specific cleavage by these constructs. By altering the nucleotide sequence within the IGS, it should be possible to design Endo.P ribozymes capable of cleaving any given single-stranded RNA. The potential to target the destruction of particular RNAs makes Endo.P a viable reagent for gene

therapy through the cleavage of cellular and viral RNAs (Rossi & Sarver, 1990; Altman, 1993). Additional work is now in progress to examine the feasibility of this system.

## ACKNOWLEDGMENT

We thank Jim Nolan and Tom LaGrandeur for critical comments on the manuscript and members of the Pace and Ellington labs for their helpful suggestions concerning this work. We also thank Kaijun Li for constructing pPT332, Bernadette Pace for providing T7 RNA polymerase, Dave Waugh for providing *Fok*I, and Elizabeth Haas, Bong-Kyeong Oh, and Tom LaGrandeur for communicating results prior to publication.

## REFERENCES

Altman, S. (1993) *Proc. Natl. Acad. Sci. U.S.A. 90*, 10898–10900.

Altman, S., Kirsebom, L., & Talbot, S. (1993) *FASEB J. 7*, 7–14.

Brown, J. W., & Pace, N. R. (1992) *Nucleic Acids Res. 20*, 1451–1456.

Burgin, A. B., & Pace, N. R. (1990) *EMBO J. 9*, 4111–4118.

Clark, J. M. (1988) *Nucleic Acids Res. 16*, 9677–9686.

Davies, R. W., Waring, R. B., Ray, J. A., Brown, T. A., & Scazzocchio, C. (1982) *Nature 300*, 719–724.

England, T. E., Bruce, A. G., & Uhlenbeck, O. C. (1980) *Methods Enzymol. 65*, 65–74.

Forster, A. C., & Altman, S. (1990) *Science 249*, 783–786.

Frank, D. F., Roiha, H., & Guthrie, C. (1994) *Mol. Cell. Biol. 14*, 2180–2190.

Gold, L., Tuerk, C., Allen, P., Binkley, J., Brown, D., Green, L., MacDougal, S., Schneider, D., Tasset, D., & Eddy, S. R. (1993) in *The RNA World* (Gesteland, R. F., & Atkins, J. F., Eds.) pp 497–510, Cold Spring Harbor Laboratory Press, Cold Spring Harbor, NY.

Guerrier-Takada, C., & Altman, S. (1992) *Proc. Natl. Acad. Sci. U.S.A. 89*, 1266–1270.

Guerrier-Takada, C., Gardiner, K., Marsh, T., Pace, N., & Altman, S. (1983) *Cell 35*, 849–857.

Haas, E. S., Brown, J. W., Pitulle, C., & Pace, N. R. (1994) *Proc. Natl. Acad. Sci. U.S.A. 91*, 2527–2531.

Harris, M. E., Nolan, J. M., Malhotra, A., Brown, J. W., Harvey, S. C., & Pace, N. R. (1994) *EMBO J.* (in press).

James, B. D., Olsen, G. J., Liu, J., & Pace, N. R. (1988) *Cell 52*, 19–26.

Kikuchi, Y., Sasaki-Tozawa, N., & Suzuki, K. (1993) *Nucleic Acids Res. 21*, 4685–4689.

Knap, A. K., Wesolowski, D., & Altman, S. (1990) *Biochimie 72*, 779–90.

LaGrandeur, T. E., Hüttenhofer, A., Noller, H. F., & Pace, N. R. (1994) *EMBO J.* (in press).

Milligan, J. F., & Uhlenbeck, O. C. (1989) *Methods Enzymol. 164*, 51–62.

Nishimura, S. (1979) in *Transfer RNA: Structure, Properties and Recognition* (Schimmel, P. R., Söll, D., & Abelson, J. N., Eds.) pp 551–552, Cold Spring Harbor Laboratory Press, Cold Spring Harbor, NY.

Nolan, J. M., Burke, D. H., & Pace, N. R. (1993) *Science 261*, 762–765.

Pace, N. R., & Smith, D. (1990) *J. Biol. Chem. 265*, 3587–90.

Reich, C., Gardiner, K. J., Olsen, G. J., Pace, B., Marsh, T. L., & Pace, N. R. (1986) *J. Biol. Chem. 261*, 7888–7893.

Reich, C., Olsen, G. J., Pace, B., & Pace, N. R. (1988) *Science 239*, 178–181.

Rossi, J. J., & Sarver, N. (1990) *Trends Biotechnol. 8*, 179–183.

Segal, I. H. (1975) *Enzyme Kinetics: Behavior and Analysis of Rapid Equilibrium and Steady-State Enzyme Systems*, John Wiley & Sons, New York.

Smith, D., & Pace, N. R. (1993) *Biochemistry 32*, 5273–81.

Smith, D., Burgin, A. B., Haas, E. S., & Pace, N. R. (1992) *J. Biol. Chem. 267*, 2429–2436.

Szostak, J. W., & Ellington, A. D. (1993) in *The RNA World* (Gesteland, R. F., & Atkins, J. F., Eds.) pp 511–534, Cold Spring Harbor Laboratory Press, Cold Spring Harbor, NY.

Tallsjö, A., & Kirsebom, L. A. (1993) *Nucleic Acids Res. 21*, 51–7.

Waugh, D. (1989) Ph.D. Thesis.

Waugh, D. S., & Pace, N. R. (1993) *FASEB J. 7*, 188–195.

Woese, C. R., Kandler, O., & Wheelis, M. L. (1990) *Proc. Natl. Acad. Sci. U.S.A. 87*, 4576–4579.